

High-Power Free-Electron Lasers – Technology and Future Applications

Yehoshua Socol
Falcon Analytics, POB 82 Netanya 42100, Israel

E-mail: socol@FalconAnalytics.com

Abstract. Free-Electron Laser (FEL) is an all-electric, high-power, high beam-quality source of coherent radiation, tunable – unlike other laser sources – at any wavelength within wide spectral region from hard X-rays to far-IR and beyond. After the initial push in the framework of the "Star Wars" program, the FEL technology benefited from decades of R&D and scientific applications. Presently, there are clear signs that the FEL technology reached maturity, enabling real-world applications. E.g., successful and unexpectedly smooth commissioning of the world-first X-ray FEL in 2010 increased in one blow by more than an order of magnitude ($\times 40$) wavelength region available by FEL technology and thus demonstrated that the theoretical predictions just keep true in real machines. Experience of ordering turn-key electron beamlines from commercial companies is a further demonstration of the FEL technology maturity. Moreover, successful commissioning of the world-first multi-turn energy-recovery linac demonstrated feasibility of reducing FEL size, cost and power consumption by probably an order of magnitude in respect to previous configurations, opening way applications, previously considered as non-feasible. This review takes engineer-oriented approach to discuss the FEL technology issues, keeping in mind applications in the fields of military and aerospace, next generation semiconductor lithography, photo-chemistry and isotope separation.

1. Introduction

Free-Electron Laser (FEL) is a unique laser technology, enabling creation of tunable high-power sources. The "heart" of FEL is so called *undulator* (or *wiggler*) – a magnetic structure, creating space-alternating – but constant in time – magnetic field (see Fig. 1). High-energy electrons (delivered by an electron accelerator) wiggle due to the space-alternating magnetic field, i.e. oscillate in the transverse (to the propagation) direction, and high-frequency electromagnetic radiation is emitted. Therefore FEL is all-electric device in the meaning that, unlike high-power chemical lasers, it uses only electricity as primary power.

The term "Free-Electron Laser" was coined by John Madey [1] in 1971, who proposed FEL in its present concept. The work on devices, based on similar principles, had been already performed for decades. In 1960 Phillips [2] reported device he called "ubitron", which was essentially a microwave tube with undulator. The undulator, however, was built (and undulator radiation experimentally studied) back in 1951 by Motz [3], and even earlier in 1947 proposed by Ginzburg [4], [5].

Free-Electron Laser was first demonstrated in 1976 [6] in the infrared region. This demonstration triggered vivid interest worldwide. Very soon the military concluded, that FEL is probably the only technology, capable of achieving power levels and optical beam quality estimated to counter intercontinental ballistic missiles. Already in 1978, DARPA (US Defense Advanced Research Projects Agency) issued call for proposals, and the scientific community response

included conceptual design from Los Alamos for a 10 MW FEL [7]. Further in 1983, the field was granted relatively high funds in the framework of the Strategic Defense Initiative (SDI) in the US, and also around the globe.

The practical results of the centralized military-oriented effort were discouraging. Until 1998, only about 10 W of electromagnetic power – instead of the planned 10 MW – were available [7]. The primary reason was that then-available electron accelerators were unable to provide e-beams of sufficient quality. With the end of the Cold War, SDI was discontinued, and so was with massive investment in high-power FELs (it seems appropriate to mention in this context that though SDI failed even to approach its design goals, it posed a great political and economic challenge to the USSR and is considered by many experts to be an important factor contributing to the collapse of the latter and thus ending the Cold War. If so – we have an example how a tactical fiasco can turn into a strategic victory).

The momentum gained by the FEL science and technology was far not totally lost. The first international FEL conference was organized in 1979, and has been held on a yearly basis ever since. Back in 1977, Vinokurov and Skrinsky suggested a modification of FEL – optical klystron [8], which enabled in 1983 to achieve lasing in visible [9] and in 1989 – in UV spectral region [10]. The important achievements in the accelerator and FEL technology during the 1980-es enabled to build first user centers, exploiting the unique capabilities of FELs to produce high-brightness optical beams in IR-to-UV spectral range.

During the two decades of roughly 1990-2010, FEL research installations and user facilities were built all over the world (the number of active FEL facilities is presently estimated as about 40). Concurrently there was a steady accumulating of advances in all the three sub-fields of the FEL technology – electron injection, main electron acceleration, and FEL interaction & optics (the division is somewhat arbitrary, but logical and widely mentioned). The short-wave limit of the electromagnetic spectrum available to the FEL technology gradually expanded from initial IR in 1976 to the hard X-rays [11], [12]. The average power also gradually grew, reaching the highest demonstrated level of 14 kW at 1.6 μm in 2006, at the US Thomas Jefferson National Accelerator Facility (TJNAF) [7]. Presently there are clear signs that the FEL technology reached maturity, enabling real-world applications. E.g., successful and unexpectedly smooth commissioning of the world-first X-ray FEL in 2010 [11] increased in one blow by more than an order of magnitude ($\times 40$ – from 6.5 nm down to 0.15 nm) the wavelength region available by FEL technology, and thus demonstrated that the theoretical predictions just keep true in real machines. Experience of ordering turn-key electron beamlines from commercial companies [13][14] is a further demonstration of the FEL technology maturity (both facilities achieved first lasing in 2011). Moreover, successful commissioning of the world-first multi-turn energy-recovery linac in 2009 [15] demonstrated feasibility of reducing FEL size, cost and power consumption by probably an order of magnitude in respect to previous configurations, opening way applications, previously considered as non-feasible. In this review we concentrate on future applications of high-power FELs – in the fields of military and aerospace, next generation semiconductor lithography, photo-chemistry and isotope separation.

There exists vast literature on FELs, including monographs and review articles. However, most of them are, so to say, "for internal consumption" of the FEL community. This review, alternatively, takes an engineer-oriented approach and is meant to serve as a technology primer for a wider audience. For more details the reader is referred to comprehensive recent reviews [7] and [16]. For deeper understanding, the classical textbook of Charles Brau [17] is recommended.

2. FEL basics

Speaking about the FEL technology, we should make two remarks from the very beginning.

First, though called "laser", FEL is essentially a big electron-beam vacuum device with many similarities to well-known traveling-wave tubes (TWT).

Second, though optical or even hard X-ray radiation is emitted, the FEL is fully described by classical electrodynamics and (relativistic) mechanics.

In Free-Electron Laser (FEL), electron beam is created by electron gun, accelerated by *Electron accelerator* (figure 1), bended by a set bending magnets and injected into the *undulator* (or *wiggler*). The electrons wiggle due to the undulator space-alternating magnetic field, i.e. oscillate in the transverse (to the propagation) projection, and high-frequency electromagnetic radiation is emitted. In oscillator configuration, the simplest optical (laser) resonator consists of two mirrors – one almost totally reflecting (*Reflecting mirror*) and one semi-transparent (*Out-coupling mirror*). Due to positive feedback, the radiation power increases from the initial noise level to the level of saturation.

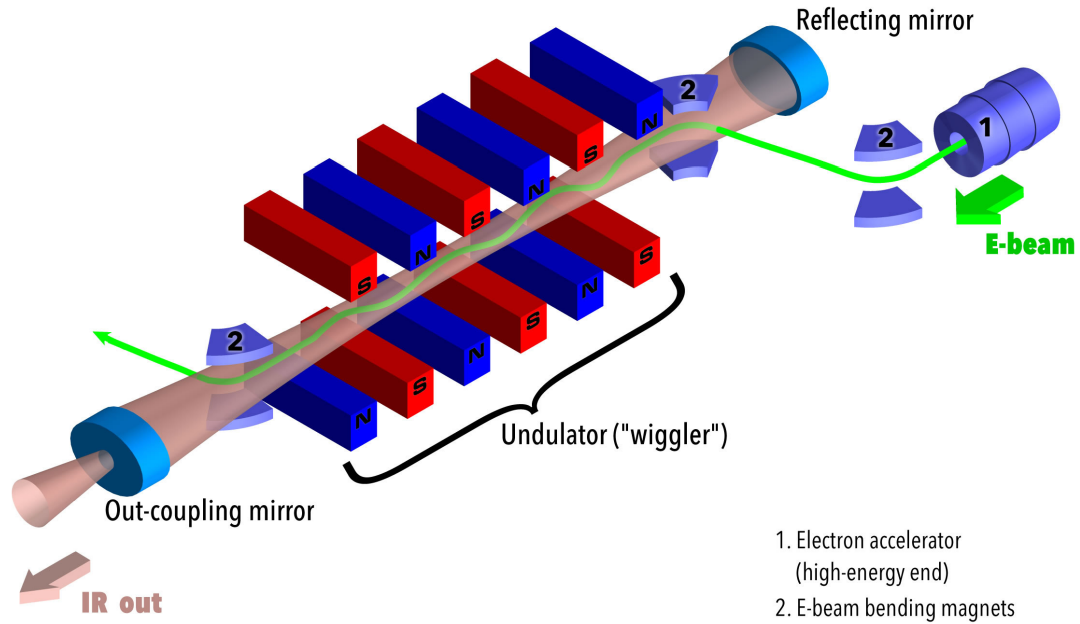


Figure 1. General IR-FEL lay-out.

The FEL radiation wavelength is usually by orders of magnitude shorter, than the undulator period. The connection between the electron beam speed and the FEL radiation wavelength (synchronism condition) is similar to that of microwave devices (for example, TWT) and is illustrated at figure 2.

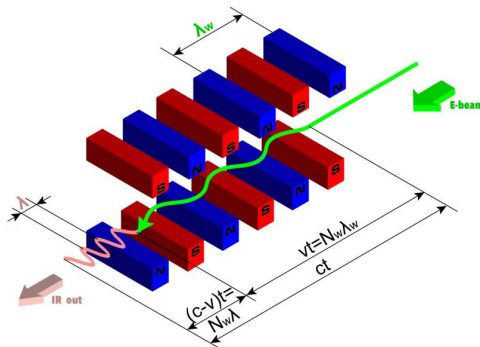


Figure 2. The connection between the electron beam speed and the FEL radiation wavelength (synchronism condition) is similar to that of microwave devices like TWT.

The synchronism condition is

$$\lambda = \lambda_w (c - v) / v, \quad (1)$$

where λ_w is the undulator period and c, v are speeds of light and of the electrons, correspondingly.

Defining $\beta=v/c$, we have

$$\lambda = \lambda_w (1 - \beta)/\beta = \lambda_w (1 - \beta^2) / [\beta(\beta+1)]. \quad (2)$$

For ultra-relativistic beams, $c - v \ll c$ and therefore $\beta \approx 1$, and taking into account relativistic kinematics we can write

$$\lambda = \lambda_w / 2\gamma^2 \quad (3)$$

where $\gamma=(1 - \beta^2)^{-1/2}$ is the Lorentz-factor $\gamma = E(\text{particle}) / mc^2$, m is the electron rest mass. Numerically, $mc^2 = 0.511 \text{ MeV}$ and correspondingly $\gamma \approx 2 \times E[\text{MeV}]$.

This basic formula should be corrected to take into account the reduction of the electron average velocity due to wiggling in the undulator's magnetic field. Taking into account this correction, the wavelength λ can be estimated according to [17]

$$\lambda = \lambda_w (1 + K^2/2) / 2\gamma^2 \quad (4)$$

where K is the dimensionless undulator parameter. The formula for K (in SI units) is

$$K = e B_u \lambda_w / 2 \pi m c \quad (5)$$

B_u is the magnetic field amplitude along the undulator axis, e and m are the electron charge and mass correspondingly. By substituting the values of e , m and c , formula (2) can be written in a way convenient for calculations

$$K=0.093 \cdot B_u[\text{kGs}] \cdot \lambda_w[\text{cm}] \quad (6)$$

For most applications, $K \sim 1-2$, but may be sometimes much more (for LCLS, e.g., $K \sim 3.7$).

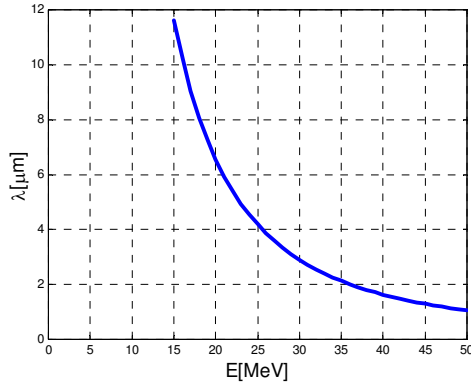


Figure 3. IR wavelength λ as a function of the electron-beam energy. Undulator period $\lambda_w = 2 \text{ cm}$, undulator parameter $K=1$. Since $mc^2 \approx 0.511 \text{ MeV}$, $\gamma \approx 2 \times E[\text{MeV}]$.

As any other laser, FEL can be realized either as a (single-pass) amplifier or as an oscillator (radiation build-up due to positive feedback). At present, due to various system considerations probably all existing infrared-terahertz (IR-THz) FELs are oscillators, while all short-wavelength machines are amplifiers. In oscillator configuration, the optical beam is formed by the surrounding (resonator) optics. Practically, 20% single-pass amplification (so called *low-gain regime*) is usually enough. In amplifier configuration, the optical beam is guided by the electron beam. The latter demands high electron currents (usually 100A or higher), and high single-pass amplification of 10^3 or even much higher. Actually, this is high amplification that provides optical guiding by the electron beam (*high-gain regime*). Due to that connection between high-gain regime and amplifier configuration, high-gain oscillator configuration is called in FEL jargon *regenerative amplifier* [18]. Regenerative amplifier is considered perspective solution for high-power FEL [7].

Among the advantages of the FEL technology one should mention:

1. Tunability across the electromagnetic spectrum from RF S-band (3-cm free-electron masers, probably of purely academic interest) to hard X-rays (0.08 nm – present record, achieved in 2011 at SACLA facility, Japan [12]).
2. Excellent optical beam quality – up to 90% of energy in the fundamental mode (the corresponding beam quality factor $M^2 \approx 1.05$). The bandwidth may be 10^{-3} and less.
3. High peak power – 1-10 MW and above (up to 10 GW at LCLS).
4. All-electric device with long life, like solid-state and fiber laser, unlike existing high-power gas lasers.

The present challenges include:

1. No industrial experience – existing FELs function as scientific user facilities.
2. Low efficiency. The present wall-plug efficiency is at 1-2% level, with 10% being a reasonable goal, still to be reached.
3. Size and cost: the smallest of present FELs have room-scale footprint and ~10 M\$ price tag, while both may be optimized by proper design and mass-production.
4. Presence of ionizing radiation, demanding additional logistics and making FEL technology subject to radiation regulation.

3. Technology Status

Presently, the FEL field is expanding, with new machines being built or planned in Germany (European facility XFEL), UK, Netherlands, Japan and more.

There are two rather different directions in the FEL field:

1. Infrared-terahertz (IR-THz) facilities, covering the spectral region of roughly 3 μm (mid-IR) up to 1500 μm (0.2 THz).
2. Short-wavelength facilities, covering the spectral region of roughly 200 nm (VUV) down to 0.12 nm (hard X-rays).

Among the functioning IR-THz FELs, one should probably mention first the most mature FELIX facility (Netherlands), serving the scientific community for about 20 years [19],[20]. There are also FEL user facilities at TJNAF (US) [21], HZDR (Germany) [22], CLIO (France) [23], Budker INP (Russia) [24] and others.

Short-wavelength machines include LCLS at SLAC (US) [25], SACLA (Japan) [26], FLASH at DESY (Germany) [27], FERMI (Italy) [28], OK-5 at Duke U. (US) [29] and more.

During the last two decades, after successful commissioning of the first FEL user facilities, considerable progress has been achieved. This progress manifests in improved reliability and decreased costs. Table 1 below lists the progress in different areas of the FEL technology, classified into three main fields: electron injection, electron acceleration and FEL interaction. The reliability progress is mainly due to the progress in the fields of RF sources and of e-beam control. Cost-down – present and future – primarily due to development of energy-recovery, multi-turn acceleration, RF sources and control hardware (electronics).

We would like to point out four signs that testify in our opinion about the FEL technological maturity.

First, as just mentioned above, many FEL machines are functioning around the globe, and many more are planned. The recently-commissioned facilities include FLARE (Netherlands) [13], FHI (Berlin) [14], ALICE (UK) [30] and more in the IR-THz range. Several short-wavelength facilities are in construction worldwide: European XFEL [31], SwissFEL (Switzerland) [32], MAX-IV (Sweden) [33], PAL X-FEL (Korea) [34] and more.

Second, the smooth commissioning of the world-first X-ray FEL LCLS at SLAC, which increased in one blow the spectral region available to the FEL technology (λ down to 0.15 nm, the

previous record had been $\lambda \geq 6.5$ nm at FLASH), meant that there are no hidden issues within the technology. Recent commissioning of SACLA 0.12-nm FEL just strengthens this statement.

Third, in 2009 the US Office of Naval Research decided to move the Navy FEL program from the research field (at TJNAF) to the industry (Boeing) [35].

Last but not least, the new experience of ordering turn-key electron beamlines from industrial companies – by FLARE from RI Research Instruments GmbH [13] and by Fritz Haber Institute Berlin (FHI) from Advanced Energy Systems, Inc. [14].

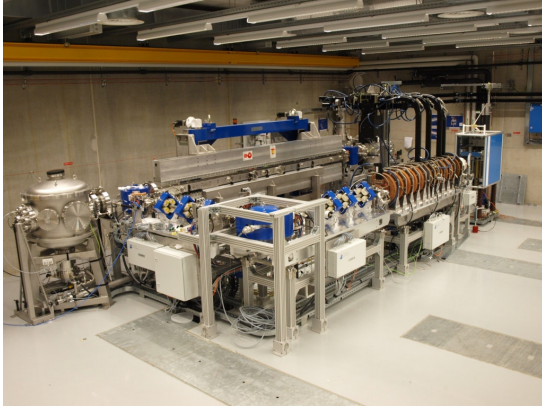


Figure 4. FLARE THz FEL at Radboud University, Nijmegen, Netherlands. Wavelength region 0.1 – 1.5 mm [13]. Courtesy RI Research Instruments GmbH – sub-contractor of the electron accelerator.



Figure 5. IR-THz FEL at Fritz Haber Institute (Berlin). Turn-key electron beamline was supplied by Advanced Energy Systems, Inc (AES). Wavelength region 0.004 – 0.4 mm [14]. Courtesy AES.

Sub-system	Progress	
Electron injection	Considerable	<p>Photo-injection</p> <ul style="list-style-type: none"> • Emergence of technology • Commercialization of driving laser systems <p>Thermionic-cathode e-guns</p> <ul style="list-style-type: none"> • Development of schemes with low emittance; • Further commercialization of high-current cathodes <p>Design software: commercialization (GPT, ASTRA)</p>
Electron Acceleration	Major	<p>e-beam dynamics</p> <ul style="list-style-type: none"> • Full description by simulation software • Commercialization of simulation codes (PARMELA, GPT, ELEGANT). <p>e-beam control</p> <ul style="list-style-type: none"> • Hardware and software: emerging and commercialization of new generation of electronics • Further development of streak cameras, photodiode matrices, low-noise amplifiers <p>New configurations</p> <ul style="list-style-type: none"> • Energy recovery • Multi-turn acceleration with energy recovery <p>Accelerating structures</p> <ul style="list-style-type: none"> • Superconducting accelerating structures – development • Commercialization – super- and normal-conducting • Development of laser trackers (alignment) <p>RF sources</p> <ul style="list-style-type: none"> • Further development of accelerator-specific RF sources • Emerging of solid-state RF sources • Development of DC current sources (pulsers)
FEL interaction & Optics	Considerable	<p>FEL physics</p> <ul style="list-style-type: none"> • Full understanding (e.g. GENESIS code) <p>Undulators</p> <ul style="list-style-type: none"> • Further commercialization • Development of the superconducting (SC) technology, including coolers and high-temperature SC input leads • Development of magnetic materials • New mechanical designs <p>Optical resonators</p> <ul style="list-style-type: none"> • Development and commercialization of heavy-duty mirrors (up to 10MW/cm² CW in IR) • Development of multi-layer Mo/Si mirrors for EUV lithography

Table 1. FEL progress 1990-2010.

4. Technology I – Electron beam delivery

4.1 RF Linac

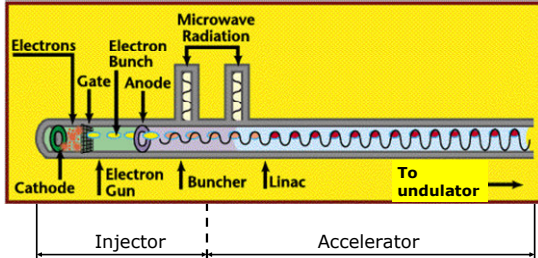


Figure 6. RF-linac layout. Courtesy APS at Argonne National Laboratory.

Radio-frequency linear accelerators (RF linacs) have special place in FEL technology. At present, this is the only technology that enables to obtain electron beams of relevant energy and current for high-power applications.

The basic idea of an RF linac is illustrated schematically in figure 6. The accelerator itself consists of series of resonant cavities in which an RF electromagnetic field is oscillating. Electrons pass the subsequent cavities, and the timing of their arrival is synchronized with the direction and phase of the RF field in each cavity – so that the energy of each electron increases from cavity to cavity. Typically, the resonant frequency is of the order of 1 GHz (L-band) or 3 GHz (S-band), though may be considerably lower (180 MHz at Budker INP FEL [24]) or higher (12 GHz at the future CLIC accelerator [36]). The electromagnetic (EM) field oscillating in each cavity has an electric field parallel to the axis which is used to accelerate the electrons. As electrons pass from one cavity to the next, their arrival is to coincide with the maximum of the oscillating electric field in each cavity. The RF power required to build up and sustain the EM field is supplied by an external power source, usually high-power *klystron* (driven by a high-voltage DC source – *modulator*), and distributed from cavity to cavity by internal coupling.

The accelerating cavities can be normal-conducting ("warm") or superconducting (cryogenic). The two schemes are compared in sec. 7.3 below. The average accelerating gradient is usually 10-30 MeV/m. E.g., the half-century-old SLAC accelerator with S-band warm accelerating cavities has average accelerating gradient of about 17 MeV/m (50 GeV over 3 km) [37]. Warm accelerating structures at higher frequencies of the accelerating RF field enable higher accelerating gradients – e.g., the design value for CLIC is 100 MeV/m at 12 GHz [CLIC].

Due to the very basic feature of accelerating by an oscillating field, RF linac output consists of single bunches (*micropulses*), their duration being a fraction of the oscillating field period. E.g., for S-band with period of $\sim 300\text{ps} = (3\text{GHz})^{-1}$, typical micropulse duration is below 20 ps. Train of micropulses (*macropulse*) can be theoretically infinite in time, but practically is limited by the driving klystron pulse length: typically 5-20 μs for S-band normal-conducting linacs, and much longer (1ms and more, or even CW operation) for L-band superconducting linacs. RF linac e-beam structure is illustrated at figure 7. The implications of this pulse structure on the FEL operation are discussed further.

Electron beams are collimated, bended etc. usually by magnetic fields, created by electro- or permanent magnets. These magnetic devices (rarely – electrostatic), governing the e-beam propagation, are called *electron-optic* devices. *Electron optics* has some similarity to the classical light optics in terms of mathematics, but in general comprises a separate field of knowledge. This field is extensive and well established, and the interested reader is referred to the classical textbook of Reiser [38].

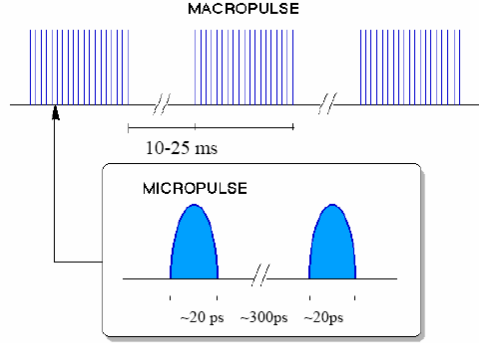


Figure 7. Electron beam structure of S-band (3 GHz) RF Linac. Electrons come in ~20ps-long *micropulses*, which are grouped into several- μ s-long *macropulses*. Courtesy FELIX.

4.2 Electron beam energy spread

As mentioned above, in RF-linac electron pulses must be short compared to the RF period in order to fit the maxima of the oscillating electric field. Assuming Gaussian shape of this pulse with phase (θ) r.m.s. σ_θ (figure 8 bottom), we can connect the peak current I_{\max} with the average macropulse current I_{av} . Namely, the total charge $I_{\text{av}} \cdot T$ ($T=1/f$ is the RF frequency) is distributed within Gaussian shape: $I(\theta) = I_{\max} \exp(-\theta^2 / 2\sigma_\theta^2)$, and the total bunch charge is calculated as $\int I(\theta)d\theta (T/2\pi) = I_{\max} \times T/2\pi \times \int \exp(-\theta^2 / 2\sigma_\theta^2) d\theta = I_{\max} \times T \sigma_\theta / (2\pi)^{1/2}$.

Since the total charge is conserved, we get

$$I_{\max} = I_{\text{av}} (2\pi)^{1/2} / \sigma_\theta \quad (7)$$

The accelerating electric field of RF linac has cos-like shape in time. If the electrons are accelerated at constant phase of the RF field from cavity to cavity of the accelerating structure, their energy is proportional to the electric field at the appropriate phase. Therefore, Gaussian distribution of electrons' phases lead to highly-asymmetrical energy spectrum with a spike at the highest energy (corresponding to the amplitude of the electric field) and exponential (i.e. rather long) tail. The corresponding spectrum shape is shown at figure 8 (top). Calculation of r.m.s. of this distribution as a function of the phase r.m.s. σ_θ of the micropulse current yields

$$\sigma_E/E = \sigma_\theta^2 / \sqrt{2}. \quad (8)$$

If the electrons are accelerated slightly off-maximum, which is often done to enable further compression of the electron bunches, the energy spread differs but the qualitative picture remains valid.

The cos-like time shape of the accelerating field is not the only (and not always the main) source of the energy spread. However, as shown just above, the electron pulses must be very short in respect to the RF period, in order that the energy spread would not be prohibitively high. It should be noted, that the energy spread of the FEL electron beam – below 1% , as shown below – should be about an order of magnitude smaller, than for most non-FEL high-energy electron-beam applications (such as cancer treatment, medical equipment sterilization etc.)

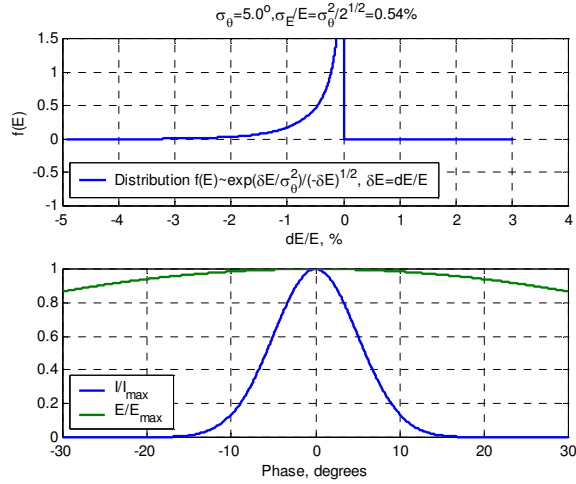


Figure 8. Electron energy spectrum (top) as a result of Gaussian pulse shape with $\sigma_\theta = 5^\circ$ (bottom).

4.3 Electron beam emittance

Due to natural spread of the angles in the electron beam, the e-beam trends to de-focus, even without electrostatic repulsion of the electrons. This trend is characterized by *emittance* ϵ . As well as the energy spread discussed in the previous section, the e-beam emittance should be considerably less than for most non-FEL high-energy electron-beam applications. The *emittance* can be defined as "area of phase space occupied by the electron distribution" [17]. The phase space $(x, x' = dx/dz)$ is 2D for each spatial dimension (x, y) , and correspondingly two "transversal" (x, y) emittances can be defined. Since electron distributions in x and y dimensions are often different, the appropriate emittances ϵ_x and ϵ_y are generally different. Emittance has dimension of length and is usually measured in units of $[\text{mm} \times \text{mrad}]$ or $[\mu\text{m}]$, which are essentially identical.

Figure 9 demonstrates propagation of electron beam with x -emittance of $1 \times \pi \text{ mm} \times \text{mrad}$. This beam has initially spatial (x) radius of 1 mm, divergence of 1 mrad (figure 9, top) and circular shape of the phase area (bottom, left). As this beam propagates (space-charge neglected), the spatial radius increases, but the phase area is preserved (being now elliptical instead of circular – bottom, right).

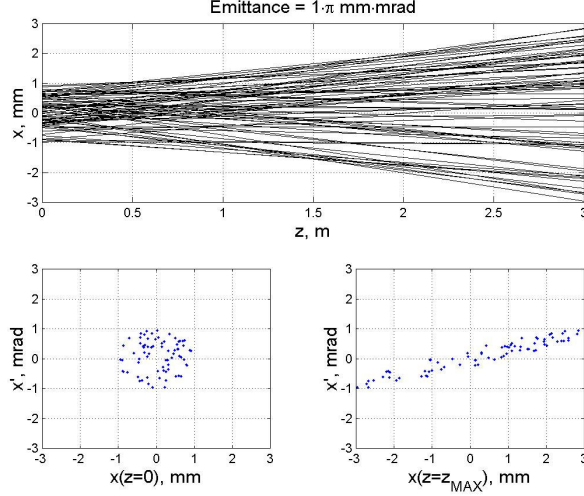


Figure 9. Propagation of electron beam with x -emittance of $1 \times \pi$ mm \times mrad. This beam has initially spatial (x) radius of 1 mm, divergence (x') of 1 mrad (top) and circular shape of the phase area (bottom, left). As this beam propagates (space-charge neglected), the spatial radius increases, but the phase area is preserved (being now elliptical instead of circular – bottom, right).

Experimentally it is difficult or just impossible to define precisely the edge of the beam (both in coordinate and direction). However, one can always define the "*r.m.s. emittance*"

$$\varepsilon_x(\text{r.m.s.}) = 4\pi [\langle x^2 \rangle \cdot \langle x'^2 \rangle - \langle x \cdot x' \rangle^2]^{1/2} \quad (9)$$

It can be shown, that for electrons distributed uniformly over circular phase-space area (as at figure 9) $\varepsilon_x = \varepsilon_x(\text{r.m.s.})$.

It comes out, that the equations governing propagation of electron beams are rather similar to the equations governing propagation of Gaussian optical beams, shortly described below in sec. 5.3. The emittance ε in electron optics plays role analogous to wavelength λ in wave optics. Not accidentally, for effective FEL interaction the electron beam must be contained within the optical beam, which leads to the condition

$$\varepsilon_{x,y} < \lambda \quad (10)$$

Unfortunately, in the literature there are several definitions of emittance. It can be defined as above, or alternatively without the factor of 4, or π , or both. Therefore one should always pay attention what is the definition used in the particular work. In the recent review [16] the r.m.s. emittance is defined as $[\langle x^2 \rangle \cdot \langle x'^2 \rangle - \langle x \cdot x' \rangle^2]^{1/2}$ and therefore the matching condition there is $\varepsilon_{x,y} < \lambda/4\pi$. It seems that the latter definition became now commonplace, at least in the field of short-wavelength FELs.

As the electron beam is accelerated, the emittance decreases; however, in the absence of space-charge and other non-uniform forces, the value $= \beta \times \gamma \times \varepsilon_x$ is generally conserved. It is called *normalized emittance*.

Normalized r.m.s. emittance is defined as

$$\varepsilon_{x,n}(\text{r.m.s.}) = \beta \times \gamma \times \varepsilon_x(\text{r.m.s.}) \quad (11)$$

$\beta = v/c$ is very close to unity for ultrarelativistic e-beams – e.g., for $E=20\text{MeV}$, $\beta=0.9997$.

Normalized r.m.s. emittance is often denoted as ε_n or just ε , leading to ambiguity. Once more, the reader should always pay attention to what stands behind the notation ε in each particular work.

4.4 Space-charge effects

Space-charge effects tend to broaden the e-beam. However, already for 20-30MeV e-beam and relevant current densities, the space charge effects are generally not too important.

The electron beam radius r_m growth due to electrostatic repulsion is described for relativistic e-beam by the following formula ([38] 4.26)

$$r_m \times r_m'' = \mathcal{K} \quad (12)$$

where $r_m'' = d^2 r_m / dz^2$ and $\mathcal{K} = eI / [2\pi\epsilon_0 m c^3 \beta^3 \gamma^3]$ (not the undulator parameter K !).

For small beam broadening, in the 1-st approximation we assume $r_m \sim \text{const} = r_0$, so r_m'' is also constant: $r_m'' = \mathcal{K} / r_0$, and after traveling distance L the beam broadening $\Delta r_m / r_0$ is

$$\Delta r_m(L) / r_0 = (I / \pi r_0^2) \times e L^2 / 4\epsilon_0 m c^3 \beta^3 \gamma^3 \quad (13)$$

figure 10 shows results for 10-cm propagation of 1A/mm² electron beam with zero emittance. Actually, for energies below 1MeV the beam spread is considerably less, than calculated by the approximate formula. However, the qualitative picture is correct: the space charge effects become less pronounced at higher energies (and practically negligible at tens of MeV), but are extremely important in injectors with electron energies below 1MeV. In general case, the effective space-charge induced angle spread $\mathcal{K}^{1/2}$ has to be compared with the beam local angle spread $\epsilon_x(\text{r.m.s.}) / [4\pi \langle x^2 \rangle^{1/2}]$. If this ratio is small, the influence of the space-charge defocusing is negligible.

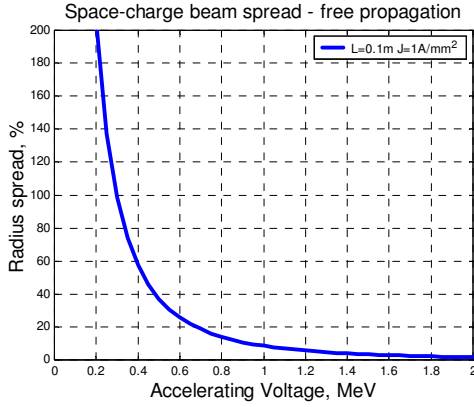


Figure 10. Electron beam spread due to space-charge at current density 1 A/mm² after 10-cm propagation with zero emittance. The space charge effects become less pronounced at higher energies (and practically negligible at tens of MeV), but are extremely important in injectors with electron energies below 1 MeV.

4.5 Electron Beam Instabilities

Many types of e-beam instabilities and other processes, deteriorating beam quality in electron accelerators, have been observed, studied and successfully treated for decades. Their description lies beyond the scope of this review and the interested reader is referred to the classical textbook of Reiser [38].

In energy-recovery linacs, which are most relevant to high-power FELs (see sec. 7.2 below), electron beam breakup (BBU) instability is of particular importance. The e-beam and the RF cavities can form a positive feedback loop that closes when the e-beam returns to the same cavity. The feedback loop can lead to BBU at sufficiently high average currents, especially for high-quality-factor superconducting cavities. The theoretical models for the BBU instability are mature and reported to be in excellent agreement with simulations and experiments. It is believed that BBU can be successfully suppressed for up to Ampere-scale currents by specially designed RF cavities [7].

5. Technology II – FEL interaction

5.1 Undulator magnetic field

Undulators are made using either permanent magnets (with or without iron poles to concentrate the magnetic field), or electromagnets (normal-conducting or superconducting). No matter what the technique is, the achievable field value decreases strongly (about exponential) with increasing the undulator gap-to-period ratio – i.e. with given undulator period, the magnetic field amplitude B_u gets weaker as the gap widens. This is an inherent property of magnetic field in undulator configurations.

It seems that the most successful and widely-used configuration is permanent-magnet undulator with iron poles. For magnets, high-coercitivity rare-earth materials like SmCo_5 , $\text{Sm}_2\text{Co}_{17}$ or $\text{Nd}_2\text{Fe}_{14}\text{B}$ are used. For poles, vanadium permendur is probably the most popular. On-axis magnetic field amplitude B_u for such undulators is often calculated according to the empirical formula [39],

$$B_u = a \times \exp[-b \times (g / \lambda_w) + c \times (g / \lambda_w)^2], \quad (14)$$

where g is the undulator gap width, $a=3.08 \times B_r$, $b=5.068$, $c=1.520$. B_r is the remnant field of the permanent magnet in units of kGs ($B_r=12$ kGs in [39]). Figure 11 shows the dependence $B_u(g / \lambda_w)$ for $B_r=13$ kGs, typical for $\text{Nd}_2\text{Fe}_{14}\text{B}$ magnets. Practically, g / λ_w ratio values of about 0.2 and higher are achievable.

The wiggling amplitude x_0 is given by ([17] 2.49)

$$x_0 = \lambda_w K / 2\pi \gamma \quad (15)$$

where $K=0.093 B_u[\text{kGs}] \lambda_w[\text{cm}]$ was defined above. For typical FELs, the wiggling amplitude is much less than the e-beam diameter.

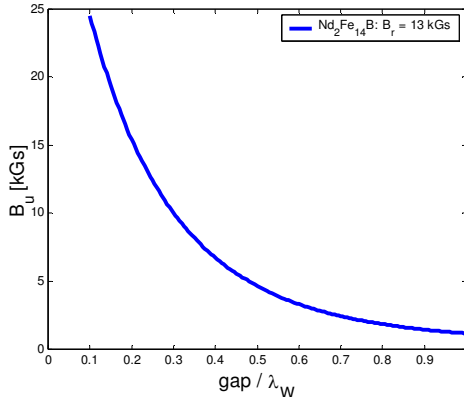


Figure 11. The dependence of the undulator on-axis magnetic field amplitude B_u as a function of the ratio (gap / undulator period λ_w) for $B_r=13$ kGs, typical for $\text{Nd}_2\text{Fe}_{14}\text{B}$ magnets. Values $gap/\lambda_w \geq 0.2$ are practical.

5.2 Matched beam, equivalent energy spread

FEL undulator, viewed as electron-optical element, has focusing properties. In modern FELs, equal-focusing undulator configuration is used. That is, focusing strength of the undulator is equal in both directions normal to the e-beam propagation.

For each combination of (e-beam emittance) and (undulator strength), there exists so-called *matched e-beam*. If the e-beam size at the entrance to the undulator is *matched* (to the undulator strength and to the e-beam emittance), the e-beam propagates as a pencil beam without convergence or divergence till the exit from the undulator.

The matched e-beam radius r_e for equal-focusing undulator is given by (see formulas 4.46, 4.14 and 4.13 of the textbook [17])

$$r_e = (\epsilon_n \times \lambda_w / K)^{1/2} / \pi \quad (16)$$

where λ_w is the undulator period, $\varepsilon_n = \beta \times \varepsilon \times \gamma$ is normalized emittance, and K – dimensionless undulator parameter.

Non-zero electron beam emittance leads to FEL gain decrease. The influence of the emittance is caused by the corresponding longitudinal velocity spread and is close to that of the e-beam energy spread. Therefore it is convenient to characterize it in terms of *equivalent energy spread*. For equal-focusing undulator, the *equivalent energy spread* $\Delta E_{\text{eq}}/E$ is given by the formula

$$\Delta E_{\text{eq}}/E = \varepsilon_n \times K / [\lambda_w (1+0.5K^2)] \quad (17)$$

(compare with [17] 4.81; there planar undulator is considered).

Formula (17) was derived in assumption of electron distribution, uniform in phase-space. $\Delta E_{\text{eq}}/E$ describes the full (not r.m.s.) energy spread. R.m.s. energy spread σ_{eq} is roughly $\sigma_{\text{eq}} \sim \Delta E_{\text{eq}}/4$.

For rather typical normalized emittance $\varepsilon_n = 30\pi$ mm×mrad (or $\varepsilon_n = 7.5$ μm , if the emittance is defined as in [16]) and relevant undulator parameters $\lambda_w = 2$ cm, $K \sim 1$, we have $\Delta E_{\text{eq}}/E \sim 0.25\%$, i.e. $\sigma_{\text{eq}}/E \sim 0.06\%$

In typical cases, this value is small regarding to the real energy spread of $\sigma_E/E \sim 0.5\%$ (see sec. 5.4 below). The influence on the FEL gain can be ignored in such cases without loss of accuracy.

5.3 Low-gain FEL

Unlike conventional lasers, light in FEL is amplified only in one way – when it co-propagates with the electron beam. Interaction of light with counter-propagating electron beam is negligible (except for some cases beyond the scope of this review).

For low-gain regime, in the so-called "cold beam" approximation – i.e. neglecting the energy spread in the electron beam – the FEL gain $G = P(\text{out})/P(\text{in})$ can be calculated according to [17] as

$$G = 1 + g_{\text{MAX}} Q L_w^3 \times JJ^2 \quad (18)$$

for low values of $G - 1$. Here $g_{\text{MAX}} = 0.135$ is numerical constant, L_w is the undulator length, and Q is given (in SI units) by

$$Q = (I/A) \times e^3 B_u^2 \lambda_w / (4\pi\varepsilon_0 \gamma^3 m^3 c^5), \quad (19)$$

where I – e-beam current, A – beam cross-section (see just below), $e = 1.60 \cdot 10^{-19}$ C – electron charge, B_u – undulator on-axis magnetic field amplitude, λ_w – undulator period; $\varepsilon_0 = 8.85 \cdot 10^{-12}$ F/m – dielectric constant, $\gamma = E(\text{beam})/mc^2$ – Lorentz-factor, $m = 9.11 \cdot 10^{-31}$ kg – electron rest mass, c – speed of light. JJ is a dimensionless factor, which approaches unity when the undulator parameter K is small. The exact value of JJ is given by

$$JJ = J_0(\xi) - J_1(\xi)$$

where J_0, J_1 are Bessel functions and $\xi = K^2 / 4(1+K^2/2)$

Few words need to be said here about the effective beam cross-section A in (22). In FEL, the e-beam and the radiation beam propagate simultaneously and interact. The interaction strength (and therefore the gain) depends on the power density of the radiation, averaged over electrons.

Therefore the relevant parameter for FEL gain calculation is the electron current density I/A , as explicit in (22). Here A – the beam cross-section – is the larger of $A(\text{e-beam})$ and $A(\text{IR-beam})$. For IR FEL – usually operated in low-gain regime – $A(\text{IR-beam})$ is often larger than $A(\text{e-beam})$, and therefore limiting the gain. Its estimation is given below in section 6.3.

The expression for Q can be rewritten in a more compact form as

$$Q = \left(\frac{I}{I_A} \frac{4\pi^2 K^2}{\lambda_w \gamma^3} \frac{1}{A} \right), \quad (20)$$

where the constant $I_A = 4\pi mc / \mu_0 e \approx 17$ kA is called *Alfven current*.

For final energy spread of the electrons ("warm beam"), the FEL gain is calculated by integrating the product of gain-curve $g(E)$ and energy-distribution (spectrum) $f(E)$, over the energy:

$$g(\text{eff}) = \int g(E) f(E) dE \quad (21)$$

The interested reader is referred to the textbook of Brau [17] for the details. Calculation of this convolution is illustrated by figure 12. It should be noted that linac spectral distribution (Fig 12, blue line) leads to higher gain in comparison to Gaussian-shape spectral distribution of the same

r.m.s. The positive branch of the gain-curve (green), or undulator spectral bandwidth, is about $1/(2N_w)$, therefore the electron energy spread should be much narrower:

$$\Delta E/E \ll 1/(2N_w). \quad (22)$$

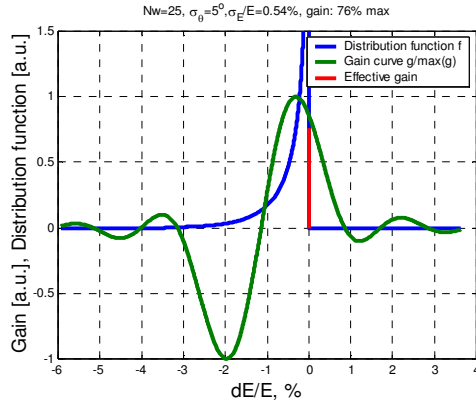


Figure 12. The FEL gain is calculated by integrating product of the gain curve (green) and the energy distribution (blue), over the energy. The undulator spectral bandwidth (positive values of the gain) is about $1/(2N_w)$. The electron energy spread should be $\Delta E/E \ll 1/(2N_w)$.

According to (21), the FEL gain g increases sharply with the undulator length L_w as $g \sim L_w^3$. However, there are at least three factors that make this dependence less sharp, and therefore enable reasonable shortening of the undulator.

- 1) As the undulator becomes shorter, the IR beam cross-section decreases increasing the gain (as described above in sec. 5.3).
- 2) As the IR beam cross-section decreases, the undulator gap can be done narrower, increasing the magnetic field (B-field) and therefore increasing the gain (sec. 5.1).
- 3) Shorter undulator is less prone to gain reduction due to the e-beam energy spread and emittance: with less undulator periods N_w , the gain curve width $1/(2N_w)$ increases (as just described above).

FEL optical power P can be estimated (in the oscillator configuration) by the fraction of the electron beam power $I \times E/e$ that spans the undulator spectral bandwidth, $1/(2N_w)$,

$$P = \eta \times I \times U = I \times U / 2N_w, \quad (23)$$

where $U = E/e$ is e.g. 20 MV for 20-MeV electron beam (for electrostatic accelerator, U is the accelerating voltage plus 511 kV, corresponding to the electron rest mass).

One immediately notices that the dependence on the undulator length is opposite for the gain and for the generated optical power. Typically for IR FELs, the trade-off between the gain and the optical power yields the number of periods $N_w \sim 15-25$, and therefore the extraction efficiency $\eta \sim 2-3\%$. In fact, the significant part of the power, extracted from the electron beam, is lost due to the optical resonator losses, as described below in section 6.1.

5.4 High-gain FEL

For high-gain regime, there is exponential dependence of the FEL gain on the length [40]:

$$G = [1/9] \times \exp(L_w/L_g) \quad (24)$$

In this case, the optical beam cross-section A in the formulas (22) and (24) above is no longer additional parameter. Within the undulator the optical beam is guided by – and matched to – the electron beam, so A is determined by the electron beam geometry. The high-gain FEL properties are described in the first approximation by so the called *Pierce parameter* ρ [16]:

$$\rho = \frac{1}{4\gamma} \left(\frac{I}{I_A} \frac{\lambda_w K^3 J J^2}{\pi^2 \epsilon_n'} \right)^{1/3} \quad (25)$$

where $\epsilon_n' = \beta \times \gamma \times \epsilon(\text{r.m.s.}) / 4\pi$, $\beta \times \gamma \times \epsilon(\text{r.m.s.})$ is normalized r.m.s. emittance as defined above in (9) and (11), K is the undulator parameter, J_J is the Bessel-function factor and $I_A \approx 17$ kA is *Alfven current*. Typical values for Pierce parameter ρ for UV/X-ray FELs are $\sim 10^{-4} - 10^{-3}$. The gain length is given in the first approximation (also called one-dimensional) by

$$L_g = L_g(1D) = \frac{d}{4\pi\sqrt{3}\rho}, \quad (26)$$

For better accuracy one should use Xie's parametric formula [41], which introduces correction to 3D effects.

In high-gain regime, the extraction efficiency η is $\eta \sim \rho$, and the optical power is therefore

$$P = \rho \times I \times U, \quad (27)$$

where $U = E/e$ is e.g. 20 MV for 20-MeV electron beam.

6. Technology III – Optics

Laser in general, and FEL in particular, is brought to oscillator regime by placing two mirrors, comprising optical resonator, around the gain medium (in the case of FEL – around the undulator). Usually, the power out-coupling is performed from one side only, as depicted at Fig. 1.

In this section we first discuss the general, more or less wavelength-independent issues of optical resonators and reaching saturation. Then we discuss in some details the issues specific to infrared and to extreme ultraviolet FELs – the two spectral regions of most practical interest (in our view) to high-power applications.

6.1 Saturated power and out-coupling in low-gain FEL oscillator

As electrons transmit their energy to the electromagnetic field, they are decelerated and consequently go out of synchronism with the optical wave. This limits the fraction of energy transmitted to the optical wave by the FEL interaction, leading to *saturation*. The process of saturation cannot be described analytically for practical cases, but numerical simulations yield good correspondence with the experimental results. Both experiments and simulations show, that for most of the practical cases the upper limit for the extracted FEL optical power P_0 can be roughly estimated by the fraction of the electron beam power $I \times E/e$ that spans the undulator spectral bandwidth, $1/(2N_w)$,

$$P_0 = \eta \times I \times U = I \times U / 2N_w, \quad (28)$$

where $U = E/e$.

The process of saturation can be empirically described by lowering of the FEL gain g as the optical power increases. For our purposes it will be convenient to express the FEL gain via the *extracted* optical power P_{extr} , connected with power P_{circ} *circulating* in the optical resonator by $P_{\text{extr}} = g \times P_{\text{circ}}$. In very general conditions we can write

$$g(P_{\text{extr}}) = g_0 \times f(P_{\text{extr}}) \quad (29)$$

where $f(x)$ is some function, decreasing monotonously from $f(0)=1$ to $f(P_0)=0$ at some power value P_0 . This situation is similar to the saturation processes in conventional lasers (see e.g. the classical textbook of Siegman [42]). For homogeneously-broadened lasers, the gain (expressed in terms of *circulating* power P_{circ}) is

$$g(P_{\text{circ}}) = g_0 / [1 + g_0 \times P_{\text{circ}} / P_0] \quad (29a)$$

It is immediately seen from (29a) that at high power levels $P \gg P_0$, the *extracted* power $P_{\text{extr}} = g(P_{\text{circ}}) \times P_{\text{circ}}$ saturates at

$$P_{\text{extr}} = g(P_{\text{circ}}) \times P_{\text{circ}} \rightarrow P_0, \quad (29b)$$

so P_0 is called *saturation power*. It can be readily shown that Eq. (29a) is equivalent to (29) with

$$f(P_{\text{extr}}) = 1 - P_{\text{extr}} / P_0. \quad (29c)$$

FEL, however, cannot be described as homogeneously-broadened laser and analytical expressions for the gain are not available. Nevertheless many experimental results (see e.g. [43], [44]) can be approximated to fair accuracy by the following empirical formula:

$$g(P_{\text{extr}}) = g_0 \times [1 - (P_{\text{extr}} / P_0)^2], \quad (30)$$

which is different from the homogeneously-broadened gain (29c) "only" by the substitution

$$P_{\text{extr}}/P_0 \rightarrow (P_{\text{extr}}/P_0)^2$$

E.g., Fig. 13 shows experimental data from Ref. [44] on FEL gain as a function of intra-cavity circulating power P_{circ} and extracted power P_{extr} , compared with the parametrization (30).

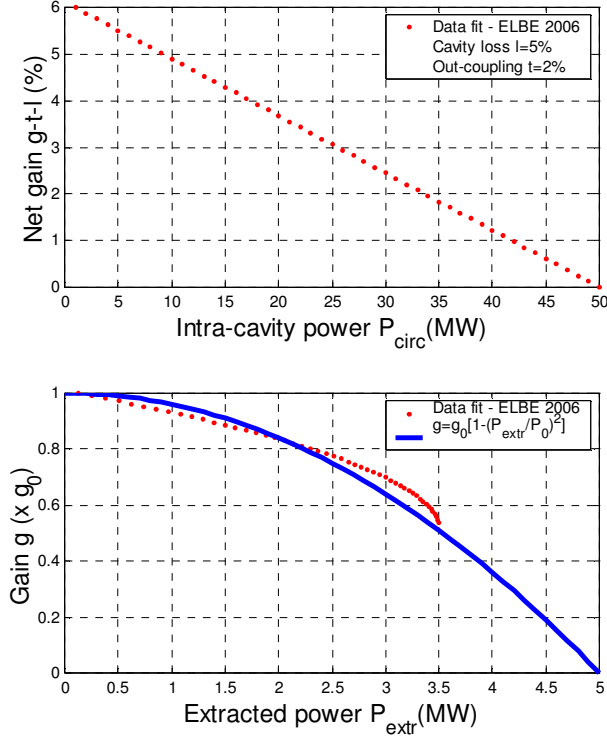


Fig. 13. FEL gain as a function of intra-cavity circulating power P_{circ} (top) and extracted power P_{extr} (bottom). Experimental data from Ref. [44] compared to the empirical formula $g(P_{\text{extr}}) = g_0 \times [1 - (P_{\text{extr}} / P_0)^2]$

Parametrization (29)-(30) is convenient since it enables to obtain simple analytical (though somewhat rough) estimations. For given optical resonator with internal losses l and power out-coupling (or transmission) t , assuming $l, t \ll 1$, in steady-state condition (gain g is equal to the total round-trip loss $t+l$) we have for the saturated value P_{extr}^0 of the extracted power:

$$g(P_{\text{extr}}^0) = g_0 \times f(P_{\text{extr}}^0) = t + l \quad (31)$$

Taking into account (30) and (31) we have simple analytical expression

$$P_{\text{extr}}^0 = P_0 [1 - (t+l)/g_0]^{1/2} \quad (32)$$

The saturated *circulating* (in the resonator) power P_{circ}^0 is much higher. Due to (31), it is connected with P_{extr}^0 by

$$P_{\text{circ}}^0 = P_{\text{extr}}^0 / (t + l), \quad (33a)$$

and the output power $P_{\text{out}}^0 = t \times P_{\text{circ}}^0$ is

$$P_{\text{out}}^0 = P_{\text{extr}}^0 \times t / (t + l) \quad (33b)$$

Just to give impression, figure 14 shows the dependence of P_{out} and P_{extr} on the out-coupling coefficient t for the gain saturation parametrized by (30). While there is still optimal value of the out-coupling t , the maximum is broader than for most conventional lasers. Practically, keeping in mind the need to keep the mirror load, i.e. intra-cavity circulating power, as low as possible, the optimal out-coupling t_{opt} is usually near the half of the net small-signal round-trip gain ($g_0 - l$) of the closed resonator

$$t_{\text{opt}} \approx (g_0 - l) / 2. \quad (34)$$

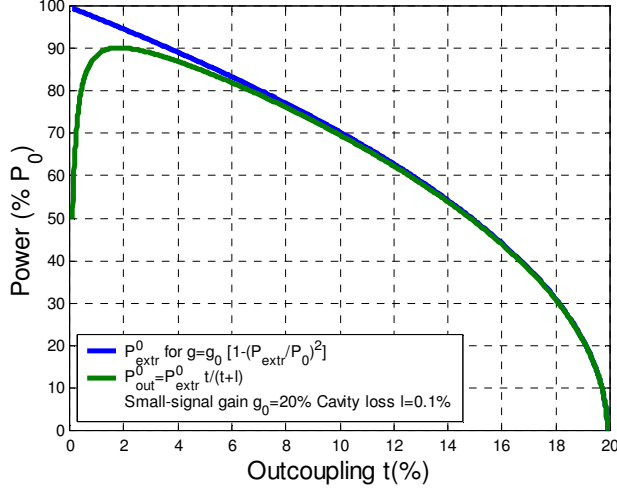


Figure 14. The dependence of output optical power P_{out}^0 and of the extracted (from the e-beam) P_{extr}^0 on the out-coupling coefficient t . The gain saturation is parametrized as $g(P_{\text{extr}}) = g_0 \times [1 - (P_{\text{extr}} / P_0)^2]$. The maximum of the saturated output power P_{out}^0 is broader than for most other-than-FEL lasers with similar parameters.

6.2 Power build-up in low-gain FEL oscillator

Electron bunches, arriving at the accelerator RF frequency, must be synchronized with the optical bunches produced by the previous electrons. Therefore, the resonator cavity round trip must be chosen as an integral multiple of [(speed of light c) divided by (the pulse repetition rate PRR)]. E.g., for the SLAC frequency $f = 2856$ MHz [37] and PRR equal to RF frequency f , $c / PRR = c / f = 10.497$ cm, therefore the resonator length L (which is half round-trip) should be therefore an integral multiple of 5.249 cm.

For FEL in oscillator configuration, the circulating in the resonator electromagnetic power grows with time – first exponentially, then linearly and finally reaching saturation after the build-up time $t(\text{build-up})$. When FEL radiation starts from noise (spontaneous emission), each electron radiates independently and the radiated power is proportional to number of electrons in e-beam bunch $n(\text{bunch})$. Near the saturation, all the electrons radiate coherently, so the electromagnetic wave field is proportional to $n(\text{bunch})$, and the power – to $n(\text{bunch})^2$. Therefore, the ratio of [saturated extracted optical power] to [spontaneous emission power] is about $n(\text{bunch})$. In typical cases (bunch charge ~ 10 -100 pCoulomb) $n(\text{bunch}) \sim 10^8$ - 10^9 . Therefore we can say that the saturation is achieved after about $\ln [P_{\text{circ}} / P(0)] / g_{\text{R-T}}$ round-trips, where $g_{\text{R-T}} = g - l - t$ is the net round-trip gain. With the round-trip time $T = 2L / c$, L being the distance between the two mirrors (i.e. resonator length), we finally have

$$t(\text{build-up}) = \frac{2L \ln[n(\text{bunch})]}{c \times [g - t - l]}. \quad (38)$$

We neglected in (38) the gain decrease near the saturation for two reasons: first, the effect of this gain decrease is rather small, since it affects only the last decade (out of 8-9, as mentioned just above) of the power build-up; second, the details of the power behavior near saturation is application-specific.

Anyhow for typical values of resonator length and FEL gain, the build-up time is of microsecond scale (see figure 15). Since commercial high-power S-band klystrons yield rather short pulses of 5-20 μs , this build-up time may be critical.

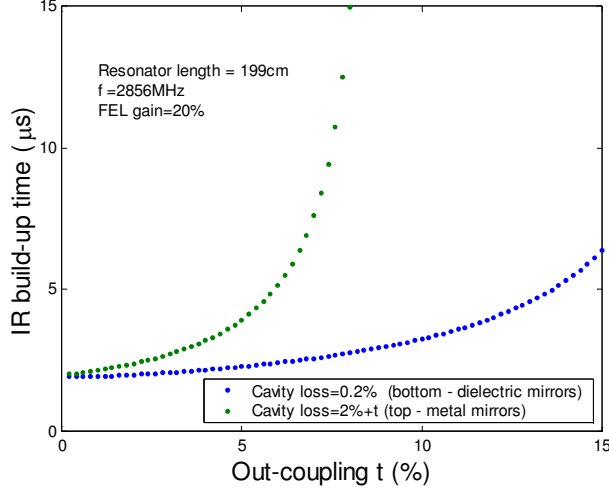


Figure 15. Build-up time for 8m-long optical resonator and 30% single-pass FEL gain. Since commercial high-power S-band klystrons yield rather short pulses of 5-20 μs , this build-up time may be critical.

6.3 Optical beam size and load estimation for high-power infrared FEL

Let us estimate now optical beam size, assuming typical for FELs Gaussian mode of IR radiation. At arbitrary position z , the Gaussian beam diameter $d(z)$ corresponding to the power level of $1/e^2$ of max (i.e. 2σ area of power) is

$$d(z) = d_0 \times \sqrt{1 + (z/L_R)^2} \quad (39)$$

where $d_0 = 2w_0$ is the IR waist diameter, and L_R is the Rayleigh length (w_0 and z_R are not independent: $\pi w_0^2 = \lambda \times L_R$). Frequently one wishes to minimize the mode size in the narrowest place of the optical resonator – the undulator. Then the Rayleigh length L_R and optimal waist radius w_0 of a Gaussian beam are related to the radiation wavelength λ and the undulator length L_{und} by

$$z_R = L_{\text{und}} / 2 \quad (40a)$$

$$w_0 = (L_{\text{und}} \times \lambda / 2\pi)^{1/2}. \quad (40b)$$

Towards the undulator ends, the beam expands up to $w = w_0 \sqrt{2}$. It should be mentioned that $w = 2\sigma$ (σ – std. deviation) of energy flux distribution in a Gaussian beam. The average (over L_{und}) $\langle 1/\pi w^2 \rangle = 1/4w_0^2$ (i.e. average cross-section is $4/\pi$ of the minimal). In the above gain estimations of Sec. 6, the IR-beam cross section should be taken as [17]

$$A(\text{beam}) = 2w_0^2, \quad (41)$$

since for a Gaussian beam with waist w the effective cross-section is given by

$$A_{\text{eff}} = \int E^2 dx dy / E(\text{max})^2 = \pi w^2 / 2 = \pi d^2 / 8 \quad (42)$$

(E is the electromagnetic field, so E^2 is the e.m. wave power density, proportional to the e.m. flux density P/A), i.e. the effective IR beam radius is $w/\sqrt{2}$.

We should note now that the waist radius w_0 also sets limits to minimal undulator gap, which must be at least $\sim 4 w_0$. In many cases this limits the magnetic field, and therefore the FEL gain.

At the resonator mirrors the beam spots are much wider. According to (39) with $z = L/2$, for the beam diameter on mirror $d(\text{mirror})$ we have

$$d(\text{mirror})=d_0 \times \sqrt{[1+(L/2L_R)^2]} \quad (43)$$

The effective beam cross-section at mirror is $\pi d(\text{mirror})^2/8$ as given by (42), so the maximal flux density at the mirror center is

$$P/A= 8P /[\pi d_0^2 \times (1+(L/2L_R)^2)] \quad (44)$$

where P is the optical power, $d_0=2w_0$ is the IR waist diameter, L is the optical resonator length (distance between the mirrors) and L_R is the Rayleigh length.

Let us take a numerical example. Assume $L_R=20$ cm, $d_0=1$ mm and $L=2$ m (these values may be relevant to some generic industrial laser). For $P_{\text{out}} = 10$ kW of output power (high-power industrial laser), assuming 10% out-coupling, we have $P=P_{\text{circ}}=100$ kW of intra-cavity power, impinging on the mirrors. The corresponding power flux P/A is about 2 MW/cm². For $P_{\text{out}}=100$ kW (US Office of Naval Research ONR prototype goal – see sec. 9.1 below) the flux density is about 20 MW/cm², and for $P=1$ MW (the design goal of the ONR program) is as high as 200 MW/cm². For longer resonator $L=8$ m, the fluxes are about 0.1 , 1 and 10 MW/cm², correspondingly. We discuss below dealing with such high values.

6.4 Mirror issues for high-power infrared FEL

Laser mirrors are either metallic or dielectric (metallic reflectors can be also dielectrically-coated). Dielectric coatings offer high reflectance, but metallic coatings operate over a broad spectral range and are more damage resistant. As a result, most IR FEL user facilities, where tuning of the FEL wavelength without changing mirrors is crucial, employ metal mirrors (usually gold-plated copper) with out-coupling via central hole. However for high-power applications on fixed wavelengths, dielectrically-coated mirrors seem preferable. IR resonator built of such mirrors will have low loss: dielectrically-coated mirrors can be produced with ppm (10^{-6}) absorption, while for metallic mirrors it is rarely somewhat below 1%. Even more important, effective radiation cross-section of the out-coupling hole is twice its area [45], so that diffractive loss is at least equal to the out-coupling. Consequently, dielectric mirrors provide much better output efficiencies and lower IR build-up time. In addition, resonator alignment is much simpler in case of dielectric mirrors, and dielectric out-coupler – unlike metal with necessary hole – can be used as a vacuum window. In FEL practice, dielectric mirrors are successfully used by TJNAF for high-power applications.

Speaking about dielectric mirrors we should mention that in the FEL environment the reflectors should bear not only dense IR flux, but also UV radiation (much weaker than IR, but considerable) inevitably produced as higher harmonics of the principal IR. This UV radiation is known to degrade the optical coatings [46],[47]. While 10 MW/cm² IR reflectors are presently commercially available [48], they are usually not stable under UV irradiation. Power out-coupling, however, comprises a grave problem, since the out-coupling element is seriously heated (this was actually the limiting factor of the TJNAF power record of 14 kW [7]).

6.5 Resonator issues for high-power Extreme Ultraviolet FEL

There are no high-reflective mirrors for the extreme ultraviolet (EUV) radiation $\lambda < 20$ nm (actually, even for $\lambda < 100$ nm). Therefore high-gain FEL regime is probably the only opportunity. In such regime the EUV beam is guided by and matched to the electron beam (within the undulator), as mentioned above in sec. 5.4.

The power density involved is rather high. Taking, after the Ref [49] value of electron beam rms radius $r_0=75\mu\text{m}$ and therefore the matched EUV beam waist $w_0=2r_0=150\mu\text{m}$, we have the Rayleigh length $L_R (\pi w_0^2 = \lambda \times L_R) L_R \approx 5.2\text{m}$. At the distance of $1 \times L_R$ from the virtual waist, the EUV beam radius is $w = w_0 \sqrt{2}$, and the effective area $\pi w^2/2 \approx 7 \times 10^4$ cm². With 5 kW CW EUV power we have power density of about 7 MW/cm². While there are, as mentioned above, IR mirrors capable of

bearing such loads [48], it is unpractical to assume that the same is achievable for EUV due to low mirror reflectivity (typically 60% or less).

Therefore there may be demand to use a ring resonator [50] as was done in the first RAFEL demonstration [51]. Mirror at grazing angle θ has potential to withstand much higher EUV power, and not only due to the $\sin(\theta)$ factor of increased area of incidence. Really, according to Fresnel formulas (Ref [52], 86.4) for refractive index $n=1+1\times 10^{-3}$ the normal-incidence reflectivity $[(n-1)/(n+1)]^2$ is about 2.5×10^{-7} , but at grazing angle $\theta=4^\circ$ the reflectivity grows to nearly 10^{-2} . The corresponding *amplitude reflectivity*, the square root of the intensity reflectivity, will be therefore 0.1, comparable with normal-incidence reflectivity in IR and visible (e.g., for $n=1.5$, normal-incidence *amplitude reflectivity* $(n-1)/(n+1) = 0.2$). This means that specially prepared multi-layer dielectric mirrors may be very effective for EUV at grazing angles. In that context positive experience with multi-layer focusing mirrors in soft X-ray region [53] is very encouraging.

Another way to eliminate the problem is to use the so-called electron out-coupling technique [54]. In this case the coherent radiation from the last section of the long undulator is used for feedback. This can be achieved in two ways [55]. Both schemes are shown in Fig. 16.

The first method uses an achromatic bend before the last undulator section. In this case, the radiation may be deflected from the main undulator axis, as shown in Fig. 16, top.

The second method (tapering) uses the last undulator section with a shorter period or a lower field amplitude. Consequently, the wavelength of radiation in the forward direction is shorter, according to Eq. (1). Therefore, the coherent radiation of the microbunched beam is synchronized with the undulator field only at some off-axis angle. The coherent radiation of the tapered section follows therefore a hollow angular distribution and can be re-circulated using a hollow mirror (Fig. 16, bottom).

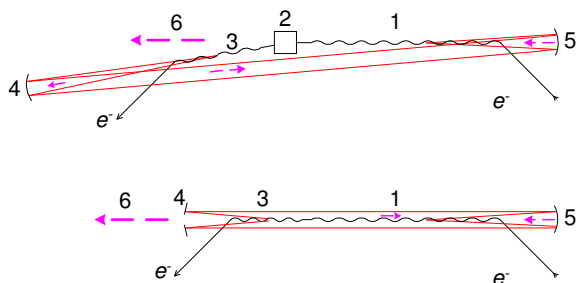


Figure 16. Two schemes of the regenerative amplifier FEL, exploiting electron out-coupling technique. Top: with e-beam bending. Bottom: with tapering. 1 – main undulator, 2 – achromatic bend, 3 – out-coupling undulator section: bended (top) or tapered (bottom), 4 and 5 – mirrors, 6 – radiation from the main undulator. Radiation used for feedback is shown by red lines and small violet arrows. Source: Ref. [49].

7. Efficiency

As mentioned above, typical extraction efficiency – the ratio of extracted-optical to e-beam power – is up to 2-3% only. The overall efficiency is further reduced due to finite efficiency of the electron beam production, the latter being further limited by the finite efficiency of RF sources (typically about 50%) and by the RF losses in the accelerator cavities (*cavity load*). Clearly, such efficiency is not acceptable for any high-power application, especially taking into account 15-30% wall-plug efficiency of modern solid-state laser technologies. In order to increase the overall efficiency, the following actions can be performed.

1. Increasing the extraction efficiency
2. Energy recovery from the spent electron beam
3. Reducing RF losses in the accelerator

We shall consider these three options separately.

7.1 Tapering

The motivation for tapering to increase extraction can be seen in the resonance condition. As the average electron beam energy decreases, electrons go out of resonance and can even consume energy from the optical field (negative gain at figure 12), beginning the saturation process. To extend resonance, one can either decrease the undulator period, bringing the electron back in resonance, or increase the undulator gap. In the latter case, which is more feasible, the undulator magnetic field and hence the value of the undulator parameter K decrease. The tapering efficacy has been demonstrated in a number of experiments and many simulations.

While tapering can be used in the amplifier to increase the extraction, the extraction is still limited to the 2-4% percent level. This is still low, and energy recovery, described further, is compulsory. However, tapering induces additional energy spread. The induced energy spread cannot be excessive and is considered to be limited to about 10-15 percent because of fundamental processes in the energy-recovery FEL.

7.2 Energy recovery

As mentioned above, only a small percentage ($\Delta E/E_0 \sim 2-3\%$) of the electrons' energy is converted into electromagnetic radiation. In energy-recovery linac (ERL), after the undulator the electron beam is bended and re-enters the linac. However, the re-entering path is designed so that the electrons' phase is π -shifted in respect to the accelerating RF field, so that the electric field now decelerates the e-beam. Its energy is therefore converted (recovered) to RF energy, substantially reducing the RF power needed to be provided (and also considerably reducing the ionizing-radiation-yield from the e-beam dump). After deceleration, the low-energy electron beam is separated from the path of the high-energy beam and directed into the beam dump.

It is anticipated, that any future high-power FEL will be driven by ERL. For ERL-FEL, 10% efficiency goal seems reasonable. Really, this goal is achieved by 2% extraction efficiency, combined with 90% energy recovery from the spent e-beam, taking into account a conservative estimation of 50% DC-to-RF conversion efficiency (with state-of-the-art up to 65%) [56].

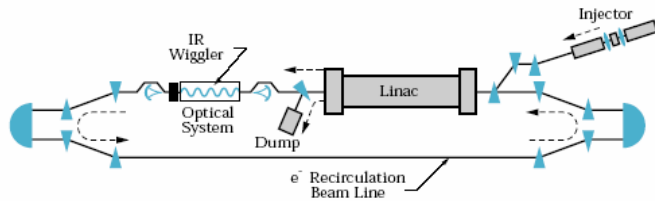


Figure 17. Principal scheme of an energy-recovery linac (ERL) driven FEL. Courtesy TJNAF.

7.3 Reducing RF losses

For normal-conducting accelerator structures, the RF losses (*cavity load*) $P(C.L.)$ are calculated by some analogue of the Ohm's law

$$P(C.L.) = U^2 / R \quad (45)$$

where $U=E/e$, E and e are the electrons' energy and charge, and $R=\Omega \times l$, with Ω being the accelerating structure *shunt impedance*. Ω depends on the RF frequency and the cavity design. The typical values are up to 60 MOhm/m for S-band linacs, down to 10 MOhm/m for larger 180-MHz cavities. The simple calculation shows that for 30MeV S-band linac of 5-m length, the cavity load is already as high as $P(C.L.)=(30 \text{ MV})^2/(5 \text{ m} \times 60 \text{ MOhm/m})=3 \text{ MW}$. We should repeat that this high power value represents the "background" load regardless the electron beam power. And this cavity load cannot be recovered. If, e.g., the FEL output IR power is taken as 100kW, the

corresponding e-beam power (with 2.5% extraction efficiency) is 4 MW. If we assume 90% e-beam energy recovery, the corresponding RF load decreases to about 0.4 MW. Compared to this, 3-MW cavity load is prohibitively high.

In order to decrease cavity load, superconductive (SC) accelerators are used (in RF fields, the heat dissipation in SC is non-zero but by several orders of magnitude lower than in normal-conducting structures). Usually, niobium (Nb) accelerating structures are used at $T=2$ K. However, such accelerators have several disadvantages:

- a) higher cost (may be by an order of magnitude);
- b) power needed for cryo-cooling (up to 50 kW continuously for each 10 MeV of acceleration);
- c) bulkiness and low robustness due to liquid helium logistics.

Another possibility is to use multi-turn acceleration (and energy recovery) with normal-conducting accelerators. Really, if we pass the electron beam twice through the same accelerating structure, the cavity load will be as low as 1/4 of the original – due to the fact that the electrons must get only 1/2 of their energy at each pass. 3-turn linac will reduce the cavity loading by factor of 9, and 4-turn – by factor of 16. The challenge of such configuration is complicated electron optics. It was estimated [57] that 4-6 turns are optimal from the point of view of the system cost. Warm (i.e. normal-conducting, not cryogenic) multi-turn energy-recovery linac was first commissioned at Budker INP in 2009 [15]. This direction seems very promising.

8. System considerations

The Committee, appointed by the US National Research Council [7], identified two main bottlenecks ("tall poles" in their own words) of the high-power IR FEL technology: electron injectors providing e-beams of high-current and high-beam-quality, and IR optics capable of bearing high power flux.

Regarding electron injection, much is invested in the photo-cathode injector technology, with UV laser used to tear electrons out of a cold cathode by photo-effect. While this technology enables to obtain multi-kA electron beams, it has severe drawbacks.

- a) Low working time – at present, up to 500 seconds (only!) at 1A current; while possibly hardly enough for military applications with seconds-long engagements, this value is prohibitively low for any industrial application.
- b) Low stand-by times – up to several weeks only, even in high vacuum. Afterwards, photo-cathode surface deteriorates and needs renewal. Unless considerably improved, this property precludes military applications.
- c) Complexity and high price tag – of M\$ scale.

Thermionic cathodes are simple, robust and mature. Their drawbacks include limited beam quality and peak current. Nevertheless, IR FELs with thermionic cathodes work for decades (FELIX, FELBE, ELETTRA). Ampere-scale average current readily achieved by thermionic cathodes is more than enough, and efforts are presently made to bunch the electron beam (i.e. to increase the peak current) up to 100A scale [58], [59].

Speaking about IR optics we should mention that in the FEL environment the optics should bear not only dense IR flux, but also UV radiation (much weaker, but considerable) inevitably produced as higher harmonics of the principal IR. As already mentioned above, this UV radiation is known to degrade the optical coatings [7]. While 10 MW/cm² IR optics is presently commercially available [48], it is usually not stable under UV irradiation. Future development will likely include, besides improving UV-stability of the gratings, incorporation of metal intra-cavity beam-expanding mirrors at grazing angles. Ring-resonator FEL with grazing-angle mirrors was proved by Dowell et al. [50] long ago.

Among additional system problems we would like to especially mention the ionizing γ -radiation, produced when high-energy electrons are intercepted by the electron-beam-line elements. E.g., taking the values of 1MW IR FEL as demanded by Navy (which translates, e.g., to 1 A current of 50-MeV e-beam and 2% extraction efficiency), state-of-the-art low interception of 10^{-4} and 10-meter distance to the crew members, yields 1R (roentgen) radiation dose during a single 10-second

pulse [60]. This comprises 20% of an annular dose permitted to radiation workers in the US (or 50% of the annular dose permitted in Europe). Radiation shielding is possible, but adds considerable weight of up to 1000-2000 kg per square meter of shielding. For lower-power applications, γ -radiation problem is less severe, but still precludes designing compact installations without significant shielding. We would mention though, that the same radiation dose of 1R comprises only 1/100 of the dose leading usually to first signs of the acute radiation syndrome.

9. Future applications

9.1 Military and aerospace

Directed-energy weapons have been pursued by military for decades. Important applications for long range lasers include the protection of ships against anti-ship missiles, of critical infrastructures against shells and rockets, and also the protection of aircrafts against surface-to-air missiles during take-off or landing. A variety of additional applications is also important, e.g. long-range remote sensing (in both terrestrial and space environment) or power transmission using laser radiation for energy delivery for unmanned aerial vehicles or even for low-orbit satellites. Moreover, laser propulsion in space is also being pursued.

Serious US military interest in FELs began in 1978, when the US Defense Advanced Research Projects Agency (DARPA) concluded that no other laser technology could yield optical beam of power and quality necessary engage strategic missiles. In 1983, the Strategic Defense Initiative (SDI) began, and tremendous progress was made in high-power FELs. In particular, the RF photoelectric injector was invented at LANL and substantial advances were made in optics. After SDI program ended about 1990, free-electron lasers were developed through programs at the Office of Naval Research (ONR). Since free-electron lasers offer the advantage of being wavelength-selectable, they can be designed to operate at optimal wavelengths in maritime environment, and even to be switched (between 2-3 options) in real time to fit the weather conditions.

Supported by ONR, researchers at the U.S. Department of Energy's TJNAF delivered the first IR light from their free-electron laser in 1998. The present record achieved (once) at TJNAF back in 2006 is average beam power of 14 kW at 1.6 μm for about 30 seconds. In order to ultimately design and build a ship-based, directed-energy weapon, the next step proposed by the Navy program is to demonstrate and study a 100 kW prototype on route to MW-class FEL. In 2009, following positive opinion of the US NRC Committee [7], ONR granted contracts to Boeing and Raytheon for preliminary design of the 100kW prototype. In 2010, Boeing received contract to finalize the design, with Los Alamos National Lab as the main subcontractor [35]. While most of the effort in the directed-energy field is invested in solid-state lasers [61], some experts believe that the potential of FEL technology is comparable to that of high-power solid-state lasers.

9.2 EUV FEL for next-generation semiconductor lithography

Optical lithography has been actively used over decades to produce more and more dense integrated circuits. To keep with the pace of the miniaturization, shorter and shorter wavelengths were used with time. The capabilities of the present 193-nm UV photolithography (with ArF laser as a source) were expanded time after time, but probably reached their physical limits. It is widely believed now that further progress will require deployment of Extreme Ultraviolet (EUV) Lithography (EUVL) based on the use of 13.5-nm radiation. However, presently there is no source available with sufficient average power to enable high-volume manufacturing. Not accidentally, several schemes for a dedicated EUV FEL for EUVL have been proposed during last years (see [62] and references therein). Two of these schemes seem especially interesting. Schneidmiller et al. [62] proposed to power scale-up the existing FLASH scheme. While this approach is expensive in the terms of capital costs, footprint and energy consumption, it is R&D-free and can be principally realized very soon. The second approach is to build a multi-turn energy-recovery separate-tracks

FEL [49]. This approach principally enables to build a cost-effective machine, but considerable R&D is still required.

The challenges of the FEL technology for the industry are absence of industrial experience and high unit price, but especially the necessity to change the fab logistics and probably the business model. Namely, the present logistics assumes dedicated light source per each lithography tool (*scanner*, or *stepper*) – and with high-price and high-power FEL, one light (EUV) source is supposed to drive multiple tools. Consequently, the business model is also to be somewhat changed. At present, the fabs just procure lithography tools (including their light sources) from manufacturers (like ASML, e.g.). FEL-based EUVL will likely demand that a separate contractor will take responsibility for the EUV source. While at present the industry does not seem to be really interested in the FEL technology due to the reasons mentioned above, this situation may change in near future if considerable progress in non-FEL EUV sources is not achieved.

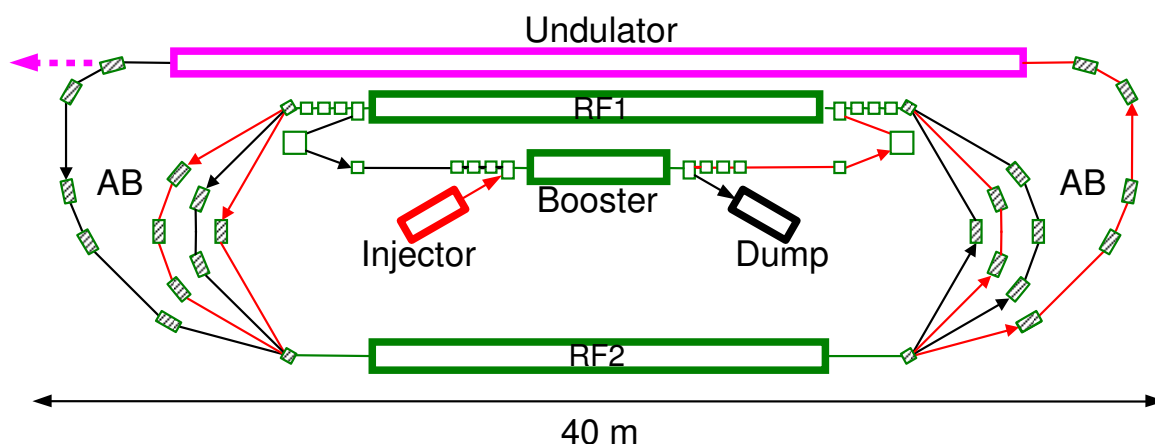


Figure 18. The scheme of energy-recovery separate-tracks FEL for extreme ultraviolet (13.5 nm) lithography. RF1 and RF2 – RF accelerating/decelerating structures, AB – achromatic bends. Red arrows – accelerating “fresh” beam, black arrows – decelerating used beam. Source: Ref. [49].

9.3 FEL for photo-chemistry

Wavelength tunability of free-electron lasers makes them intrinsically suitable for photo-chemical processing. The big advantage of photo-chemical technology is that the conditions for photo-chemical reaction chain are generally much milder, that for the appropriate purely-chemical. Namely, the involved temperatures are lower (with plant photosynthesis, e.g., evolving at ambient temperature), and amount of intermediate substances and by-products (usually toxic) – less [63]. The main challenge of photo-chemistry is high cost. Already two decades ago, two kinds of processes – both of high quantum yield (ratio of product molecules to absorbed photons) – were identified as perspective for using FELs [17]: purification of chemical compounds by removing small amount of impurities from the desired matrix, and laser-initiated chain reactions. While the entire field of industrial photo-chemistry (including laser chemistry) is not very active at present, this situation may also change in near future due to increasing demands to energy saving and pollution prevention.

9.4 FEL for isotope separation

Isotope separation is just another perspective field. From the technical point of view this application of FEL can be classified as a kind of photo-chemistry. Since different isotopes have slightly different electronic structure, free-electron lasers provide unique opportunity to target specific transitions resonantly, and therefore change chemical status of a given isotope only.

Separation of isotopes of carbon and silicon [64], boron [65], gadolinium [66] and molybdenum [67] by means of FEL irradiation was reported. Isotope engineering can be used for lowering thermal dissipation in silicon chips, producing retunable solid-state lasers, low-noise IR sensors and in many more applications [68]. However, the most volume-intensive industrial isotope separation is performed while enriching uranium for nuclear fuel [69]. The R&D in the field of uranium LIS (laser isotope separation) has been performed by decades. Recently there seems to be renewed interest in LIS, particularly *Silex* process demanding 16- μm infrared [70] – wavelength not easily obtained in high power by conventional lasers (the Los-Alamos RAFEL lased at 16 μm [51] – may be not accidentally). It is anticipated that with growing world energy demand the nuclear power industry will grow at accelerating rate (despite Fukushima). Therefore the demand for uranium enrichment (including LIS) is anticipated to increase, and FELs may find their niche.

10. Conclusions

Free-Electron Laser (FEL) technology enables to develop all-electric, high-power, high beam-quality sources of coherent radiation, tunable – unlike other laser sources – at any wavelength within wide spectral region from hard X-rays to far-IR. After the initial push in the framework of the "Star Wars" program, the FEL technology benefited from decades of research and development, leading to notable scientific applications. Presently, different FEL components become more and more commercialized, and there are further signs that the technology in general reached maturity, enabling real-world applications. Moreover, feasibility of reducing FEL size, cost and power consumption by probably an order of magnitude – in respect to present values – was also recently demonstrated.

The above considerations make relevant development of high-power applications, previously considered as non-feasible. The most probable future applications of FELs with kilowatt to megawatt power levels seem to be in the fields of military and aerospace (infrared radiation), next generation semiconductor lithography (extreme ultraviolet at 13.5 nm), photo-chemistry and isotope separation (infrared to ultraviolet).

Acknowledgements

The author wishes to thank Prof. N.A. Vinokurov (Budker INP) for his constant willingness to help, numerous extremely fruitful discussions and careful reading the manuscript. Constructive input from Prof. C. Brau (Vanderbilt U), Dr. D. Douglas (TJNAF), Mr. A. Eichenbaum, Dr. E. Gluskin (ANL), Prof. A. Gover (Tel-Aviv U), Dr. Y. Kalisky (NRC Negev), Prof. S. Litsyn (SanDisk), Dr. A. Matveenko (HZB), Dr. B.L. Militsyn (ASTeC), Dr. C. Piel (RI Research Instruments GmbH), Dr. D. Ratner (SLAC), Dr. O. Shevchenko (Budker INP), Dr. A. Shor (Soreq NRC), Dr. M. Shoval (Intel), Dr. G. Stupakov (SLAC), Dr. A. Todd (AES, Inc.), Dr. M.V. Yurkov (DESY), Dr. B. van der Geer (Pulsar Physics), Dr. A. van der Meer (FELIX), Dr. R. Wünsch (HZDR), and Dr. A. Zholents (ANL) is greatly appreciated.

References

- [1] J. Madey, J. Appl. Phys. **42**, 1906 (1971).
- [2] R.M. Phillips, IRE Trans. Elec. Dev. **7**, 231 (1960).
- [3] H. Motz, J. Appl. Phys. **22**, 527 (1951).
- [4] G.N. Kulipanov, Ginzburg's invention of undulators and their role in modern synchrotron radiation sources and free electron lasers, Physics-Uspekhi **50**(4), 368 (2007).
- [5] Гинзбург В.Л. Изв. АН СССР, Сер. физ. **11** (2) 165 (1947)
- [6] L.R. Elias, et al., Phys. Rev. Lett., **59A**, 187 (1976).
- [7] *Scientific Assessment of High-Power Free-Electron Laser Technology*, The National Academies Press, 2008. ISBN: 0-309-12690-8.

- [8] Preprint 77-59, Novosibirsk : Budker INP, 1977.
- [9] M. Billardon, et al., First Operation of a Storage Ring Free-Electron Laser, in: C. Brau (Ed.), *Free-Electron Generators of Coherent Radiation*, SPIE **453** (Bellingham, WA : SPIE, 1984).
- [10] I.B. Drobyazko, et al., Nucl. Instrum. Methods Phys. Res., Sect. A **282**, 424 (1989).
- [11] P. Emma (LCLS Commissioning Team), in *Proceedings of the 23rd Particle Accelerator Conference, Vancouver, Canada, 2009* (IEEE, Piscataway, NJ, 2009), p. 3115.
- [12] R. Tanaka et al., First Operation of the SACLA Control System in SPring-8, Proceedings of IPAC2011, San Sebastián, Spain. pp.2325-2327.
- [13] <http://www.ru.nl/FLARE>
- [14] <http://fel.fhi-berlin.mpg.de>
- [15] N.A. Vinokurov et al., Proceedings of FEL2009, Liverpool, UK, 447-451.
- [16] W.A. Barletta et al., Free Electron Lasers: Present Status and Future Challenges, Nucl. Instrum. Methods Phys. Res., Sect. A **618**, 69 (2010).
- [17] C. Brau, *Free-Electron Lasers*, Academic Press, 1990.
- [18] J. Goldstein, D. Nguyen and R. Sheffield, Theoretical study of the design and performance of a high-gain, high-extraction-efficiency FEL oscillator, Nucl. Instrum. Methods Phys. Res., Sect. A **393**, 137 (1997).
- [19] C.A.J. van der Geer et al., Performance of the FELIX accelerator, Proceedings of EPAC92, 504-506.
- [20] <http://www.differ.nl/felix/facilities/>
- [21] <http://www.jlab.org/FEL/>
- [22] <http://www.hzdr.de/db/Cms?pNid=471>
- [23] http://clio.lcp.u-psud.fr/clio_eng/clio_eng.htm
- [24] N.A. Vinokurov et al., Status and Prospects of the Novosibirsk FEL Facility, Proc. RuPAC-2010, Protvino, Russia, 2010, pp. 133-135.
- [25] http://www-ssrl.slac.stanford.edu/lcls/cdr/lcls_cdr-ch05.pdf
- [26] <http://xfel.riken.jp/eng/index.html>
- [27] <http://flash.desy.de/>
- [28] www.elettra.trieste.it/FERMI
- [29] <http://www.fel.duke.edu>
- [30] http://www.cockcroft.ac.uk/news/alice_fel.htm
- [31] <http://xfel.desy.de/>
- [32] <http://www.psi.ch/media/swissfel-the-future-project>
- [33] M. Eriksson et al., The MAX IV Synchrotron Light Source, Proceedings of IPAC2011, San Sebastián, Spain, pp.3026-3028.
- [34] S.H. Nan, Plan of PAL XFEL Project, Proc. 14 International Conference on Accelerator and Beam Utilization, October 07-08, 2010, Gyeongju, Korea.
http://www.komac.re.kr/npet/new_proton/down/conference/icabu2010/10.07_Plenary%20session/08_ICABU2010_SHNAM_101007.pdf
- [35] *Boeing to Design Free Electron Laser Lab Demonstrator*. SMT, Sep. 13, 2010.
<http://www.ems007.com/pages/zone.cgi?a=71190>
- [36] D. Schulte, CLIC Conceptual Design and CTF3 Results, Proceedings of IPAC2011, San Sebastián, Spain, p. 961-965.
- [37] R.B. Neal (Ed.), *The Stanford Two-Mile Accelerator*, NY : W.A. Benjamin, Inc. 1968.
- [38] M. Reiser, *Theory and Design of Charged Particle Beams*, Wiley-VCH 1994. ISBN-10: 0471306169
- [39] P. Elleaume, J. Chavanne, and B. Faatz, Nucl. Instrum. Methods Phys. Res., Sect. A **455**, 503 (2000).
- [40] E. Jerby and A. Gover, IEEE J. Quantum. Electronics **21**, 1041.
- [41] M. Xie, Nucl. Instrum. Methods Phys. Res., Sect. A **445**, 59 (2000).
- [42] A. Siegman, *Lasers*, University Science Books; 1st edition (1986), 1283 p. ISBN-10: 0935702113
- [43] Y. Socol et al., Phys. Rev. ST Accel. Beams **8**, 080701 (2005).
- [44] U. Lehnert et al., Proc. FEL2006, Berlin, p. 339.

- [45] L.D. Landau, E.M. Lifshitz. *The Classical Theory of Fields*, Butterworth-Heinemann; 4 ed. (1980), §61. ISBN 978-0750627689
- [46] P. Elleaume, M. Velghe, M. Billardon, and J.M. Ortega, Diagnostic Techniques and UV-Induced Degradation of the Mirrors Used in the Orsay Storage Ring Free-Electron Laser, *Applied Optics* **24**, 2762-2770 (1985).
- [47] D.A.G. Deacon, *NIM A* **250**, 283 (1986).
- [48] See, e.g., CVI Melles Griot (Albuquerque NM, USA).
<http://www.cvimellesgriot.com/Products/Tunable-Laser-Line-Mirrors.aspx>
- [49] Y. Socol et al. Compact 13.5-nm free-electron laser for extreme ultraviolet lithography. *Phys. Rev. ST Accel. Beams* **14**, 040702 (2011).
- [50] D. Dowell et al., Tests of a Grazing-Incidence Ring Resonator Free-Electron Laser, *IEEE J. Quantum. Electronics* **21**, 2613 (1991).
- [51] D.C. Nguyen et al., First lasing of the regenerative amplifier FEL, *Nucl. Instrum. Methods Phys. Res., Sect. A* **429**, 125-130 (1999).
- [52] L.D. Landau, E.M. Lifshitz. *Electrodynamics of Continuous Media*, Butterworth-Heinemann; 2 edition (1984)
- [53] A.Y. Lopatin, V.I. Luchin, N.N. Salashchenko, et al. *Technical Physics* **55**, 1018 (2010).
- [54] N.G. Gavrilov et al., *Nucl. Instrum. Methods Phys. Res., Sect. A* **304**, 63 (1991).
- [55] G.N. Kulipanov et al., *Nucl. Instrum. Methods Phys. Res., Sect. A* **375**, 576 (1996).
- [56] E.g. TH2089 1.1-MW klystron from THALES:
http://www.thalesgroup.com/Portfolio/Security/Klystrons_CW_for_Particle_Accelerators
- [57] D. Douglas et al., Proceedings of FEL2010, Malmo, Sweden, 193-196.
- [58] H. Hanaki et al. Proceedings of EPAC08, Genoa, Italy, 85-87
- [59] V. Volkov et al., Thermionic Cathode-Grid Assembly Simulations for RF Guns, Proceedings of PAC09, Vancouver, BC, Canada, 572-574.
- [60] Y. Socol, unpublished.
- [61] D. L. Carroll, Overview of High Energy Lasers: Past, Present, and Future? *42 AIAA Plasmadynamics and Lasers Conference*, 27 - 30 June 2011, Honolulu, Hawaii.
- [62] E.A. Schneidmiller, V.F. Vogel, H. Weise, and M.V. Yurkov, Potential of the FLASH FEL technology for the construction of a kW-scale light source for the next generation lithography. <http://arxiv.org/abs/1108.5986> (2011).
- [63] S. Protti et al., Photochemistry in synthesis: Where, when, and why, *Pure Appl. Chem.*, **79**, 1929–1938 (2007).
- [64] Kuribayashi S et al., Infrared multiple photon decomposition of CHBrF₂ induced by a free-electron laser, *Appl. Phys. B – Lasers and Optics* **65**, 393-398 (1997).
- [65] Hashida M et al., FEL multiphoton dissociation and isotope separation of boron, *Proc. 20th International Free Electron Laser Conference*, Williamsburg, VA : Aug 16-22, 1998. pp. 485-488.
- [66] Izawa Y et al., Researches on laser isotope separation of gadolinium and boron, *J. Nucl. Sci. Techn.* **39**, 426-430 (2002).
- [67] Noda T. et al., Isotope separation of silicon and molybdenum using a free electron laser, *J. Nucl. Materials* **307**, 715-718 (2002).
- [68] V.G. Plekhanov, Fundamentals and applications of isotope effect in solids, *Progress in Materials Science* **51**, 287-426 (2006).
- [69] P. Rigny, Present and prospective situation in laser isotope separation – will the FEL be needed? *Nucl. Instrum. Methods Phys. Res., Sect. A* **239**, 432-438 (1985).
- [70] J. Hecht, Laser uranium enrichment returns from the dead, *Laser Focus World* **47**(10), 18-20 (2011).